ON THE STELLAR POPULATION OF THE ORION NEBULA CLUSTER

Lynne A. Hillenbrand

University of California, Berkeley, CA

....poster paper presented at the Star Formation Workshop on "Star Formation in Clusters" (1996, Wellesley, MA)

Abstract:

We explore the stellar population of the Orion Nebula Cluster (ONC). Our study includes a synthesis of optical spectroscopy, optical photometry, and infrared photometry for a total sample numbering ~1600 optically selected stars located within ~2.5 pc of the namesake Trapezium stars which define the center of the ONC. Because of the large number and number density ($n_{peak} \sim 10^4$ pc^{-3}) of stars, the wide range in stellar mass ($\sim 0.1 - 50 M_\odot$), and the extreme youth (< 1-2 Myr) of the stellar population, there is no better open cluster for investigating: 1) the detailed shape of the initial mass spectrum; 2) the apparent age spread in a region thought to have undergone "triggered" star formation; 3) the time sequence of star formation as a function of stellar mass; 4) the survival time of optically thick, inner circumstellar disks, as a function of stellar mass; and 5) trends of all of the above with cluster radius. The massive stars of the ONC appear to have evacuated a cavity which extends out of the molecular cloud in our direction, rendering both the high-mass and most of the dynamically associated lower-mass stars, only slightly extincted ($A_V < 2.5$ mag). This fact enables us to study the stellar population over its full range in mass and age with an optical sample.

Approximately 30% of our total optical sample is able to be located on a theoretical HR diagram; this subsample is unbiased with respect to brightness or cluster radius, and is complete down to $\sim 1 M_\odot$. We find the ONC to be characterized by a mass spectrum which is clearly biased towards high-mass stars within the innermost radii ($r_{projected} < 0.3$ pc), but which is not inconsistent with "standard" (*e.g.* Miller-Scalo) mass spectra over larger radii. The total mass in stars is $M_{stars} < 1100 M_\odot$. We find the ONC to be characterized by an age spread which is almost strictly less than 2 Myr according to one set of pre-main sequence evolutionary tracks, but up to 5 Myr according to another set of pre-main sequence evolutionary tracks. Using either set of tracks there is a clear trend of stellar mass with stellar age (where higher-mass stars are inferred to be significantly *older* than lower-mass stars). This suggests that pre-main sequence evolutionary theory needs further refinement, particularly with respect to the feasibility of the birthline hypothesis advocated by Palla & Stahler (1993). Uncertainties regarding the accuracy of evolutionary tracks and isochrones prevent our coming to any conclusions on star formation history with mass in the ONC. Our analysis of the spatial distribution of stars reveals that the most massive stars and the youngest stars are found preferentially towards the cluster center. Furthermore, based on KS tests between cumulative mass and age distributions over different ranges, mass and age segregation appears to be a general phenomenon in the ONC. We also address cluster dynamical issues and find that since the ONC as a whole is not yet relaxed (although the inner Trapezium Cluster may be), the massive stars at the center must have formed where they are seen today, at the bottom of the potential well. Finally, we study circumstellar activity diagnostics of stars in our sample, including infrared excesses, optical emission lines (CaII triplet, OI, *etc.*), spectroscopic veiling, externally ionized nature, and stellar rotation properties. By combining our optical analysis with published and our own near-infrared photometry, we find that the fraction of stars which have retained their inner circumstellar disks to the present time is $\sim$45% averaged over the entire area of our survey. However, there are definitive trends with cluster radius of the frequency and of the magnitude of near-infrared excess, both increasing towards the cluster center. We also find a trend of near-infrared excess with stellar mass, with more massive stars significantly less likely to have excesses. We find no trend of near-infrared excess with stellar age, at least not over the limited age range in the ONC. Approximately $\sim$15% of the stars in our spectroscopic sample show broad CaII emission lines, but we find little evidence for signficant spectroscopic veiling. We find that the sources identified as being externally ionized by O'Dell and collaborators are no different from the rest of the ONC population in terms of mass, age, extinction, or near-infrared excess distributions.

The Database: Optical Stars within ∼2.5 pc of the Trapezium

- optical imaging at VI; N≈ 1600 stars
  KPNO 0.9m CCD
  HST in central region (data from Prosser *et al.*, 1994)

- infrared imaging at JHK; N≈ 700 optical + 225 infrared stars
  KPNO 1.3m OTTO for brighter stars
  KPNO 1.3m SQIID
  UMass/NICMASS

- 2 μm measurements for several thousand additional embedded sources
  OSIRIS (data from Ali & DePoy, 1995)
  MAGIC (data from McCaughrean *et al.*, 1994)

- optical spectroscopy over 5000-9000 Å ; N ≈ 450 stars
  KPNO 4m/WIYN HYDRA multiobject spectrograph
  KPNO 4m RC spectrograph with multi-slit masks
  a few spectral types from the older literature

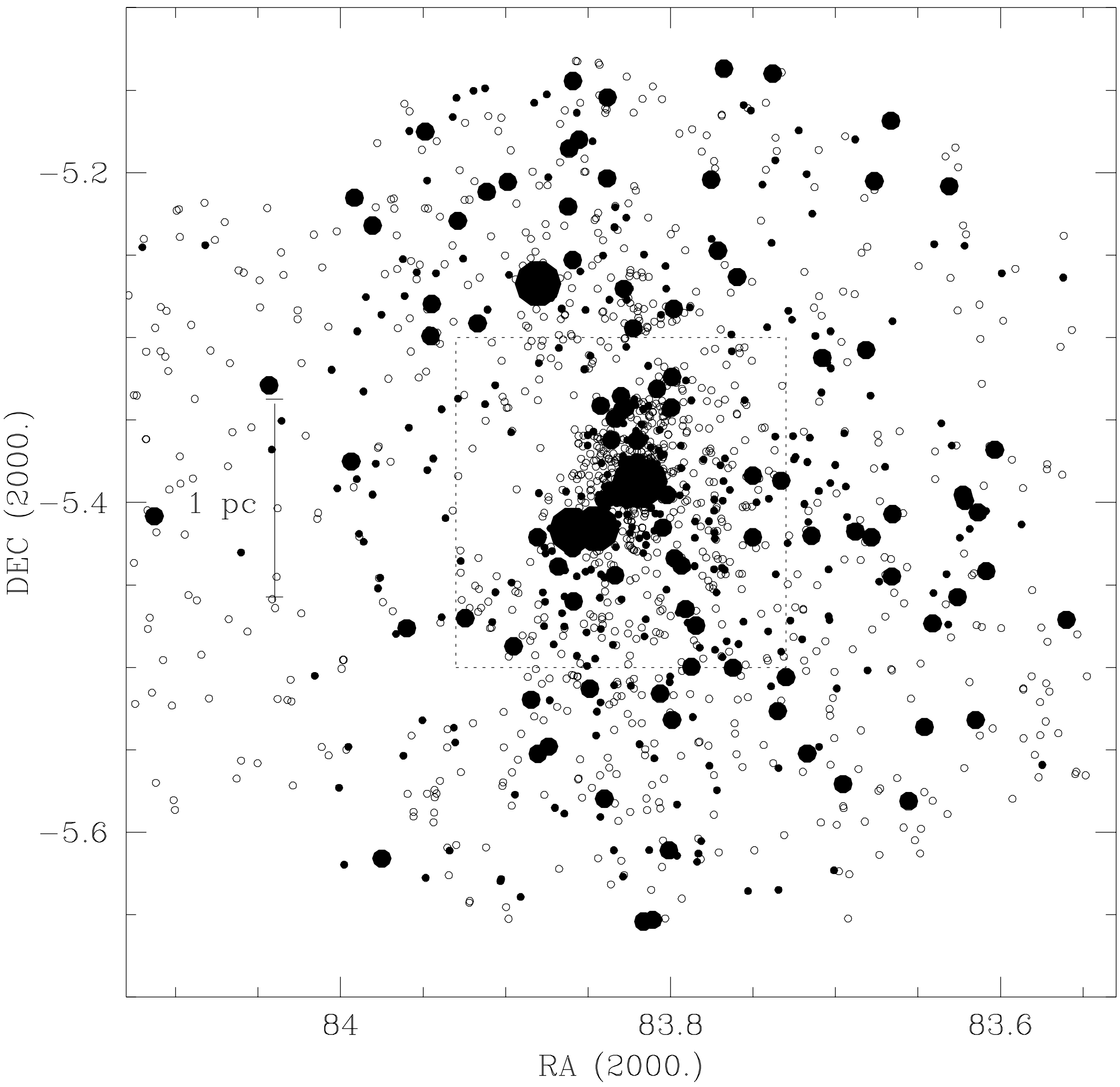

Fig. 1.— *The spatial distribution of optical stars included in this study.* Filled symbols indicate stars whose spectral types and photometry enable their location in the HR diagram. Three different point sizes indicate the stellar mass ranges: $10 < M/\ M_\odot$ (large), $1 < M/\ M_\odot < 10$ (medium), and $M/\ M_\odot < 1$ (small). Linear scale bars of length 1, 0.5, and 0.1pc are shown in panels (a), (b), and (c), respectively.

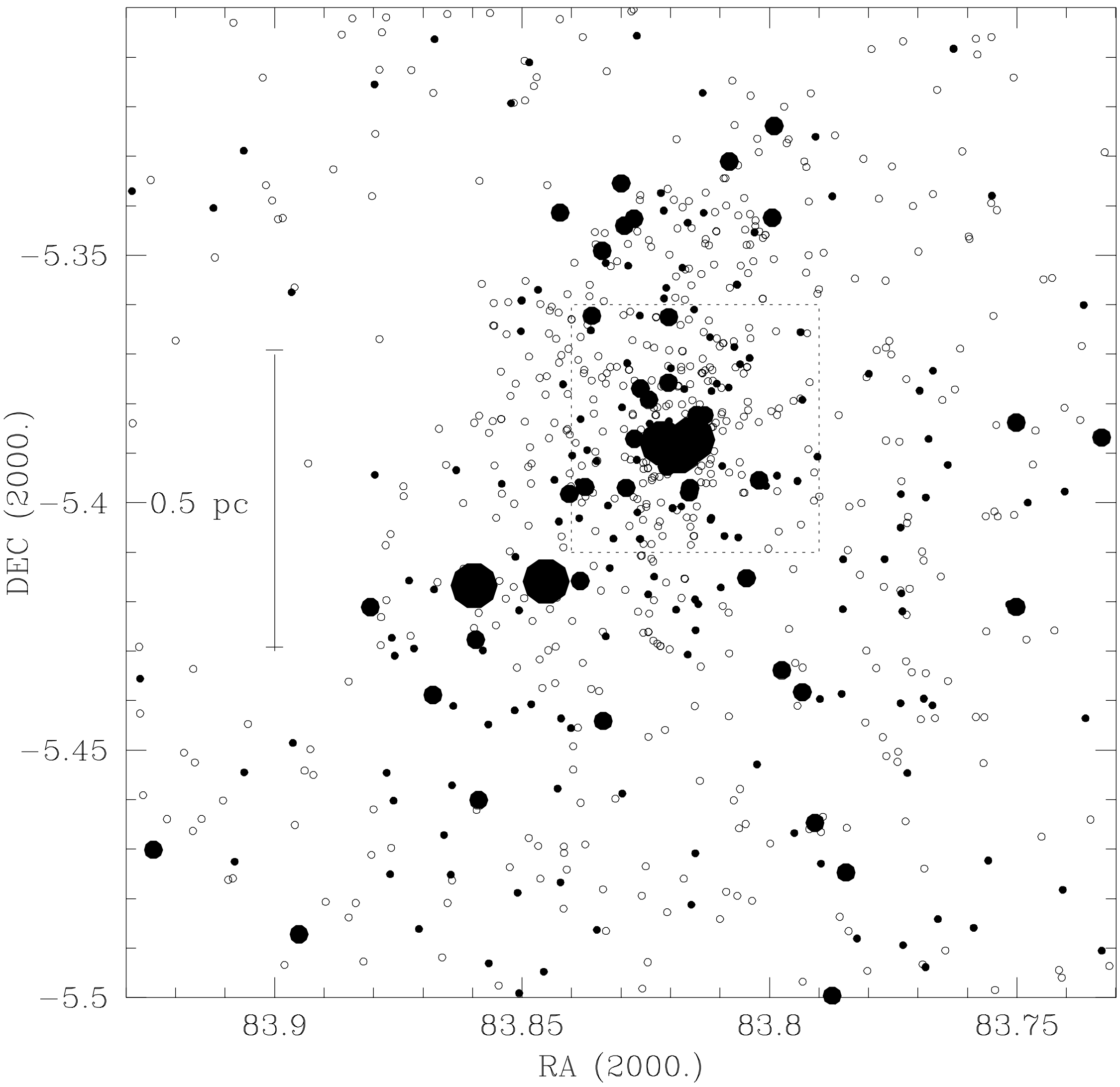

−5.35
−5.4
−5.45
−5.5
0.5 pc
DEC (2000.)
83.9
83.85
83.8
83.75
RA (2000.)

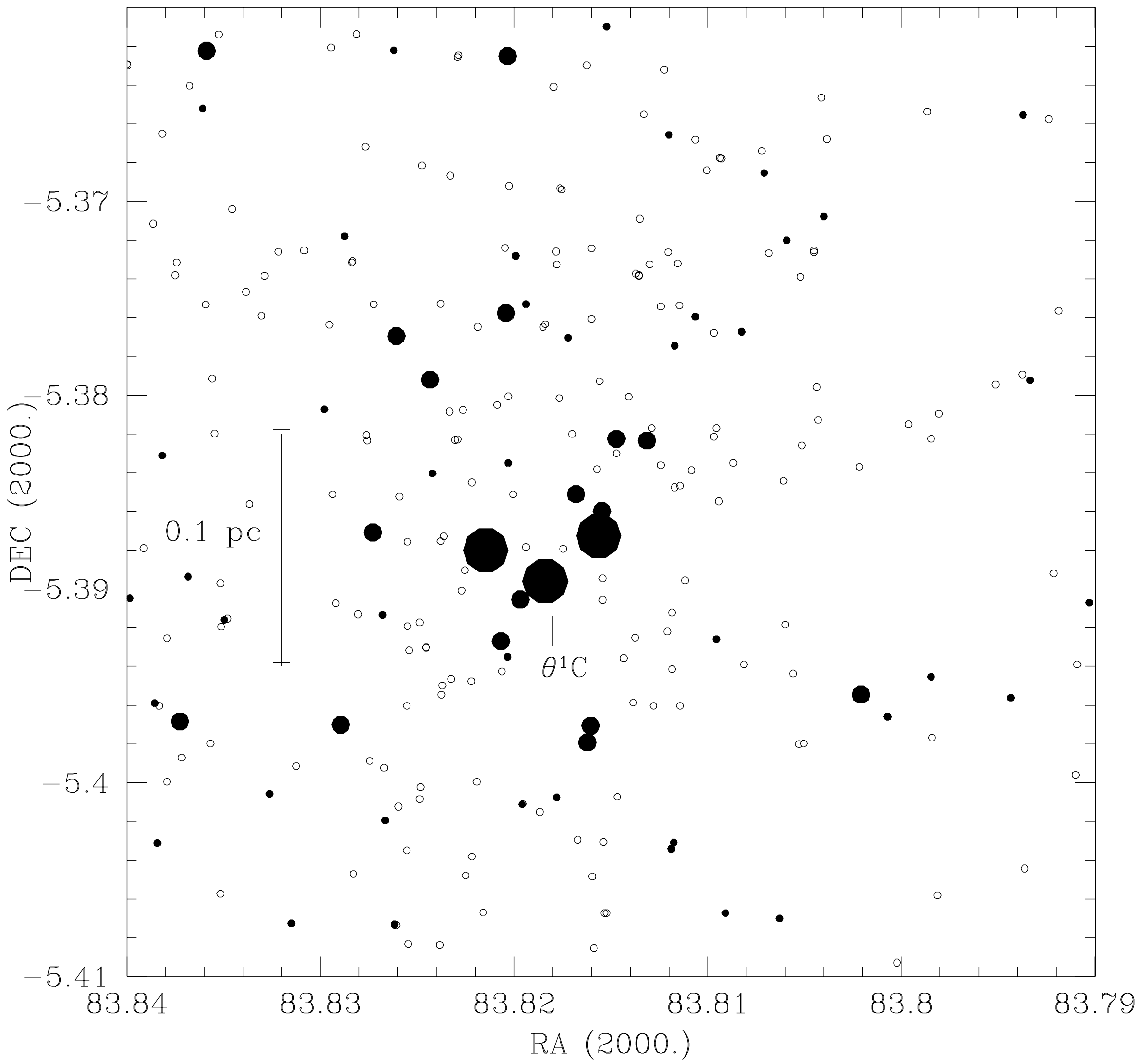

DEC (2000.)
−5.37
−5.38
−5.39
−5.4
−5.41
0.1 pc
θ^1C
83.84
83.83
83.82
83.81
83.8
83.79
RA (2000.)

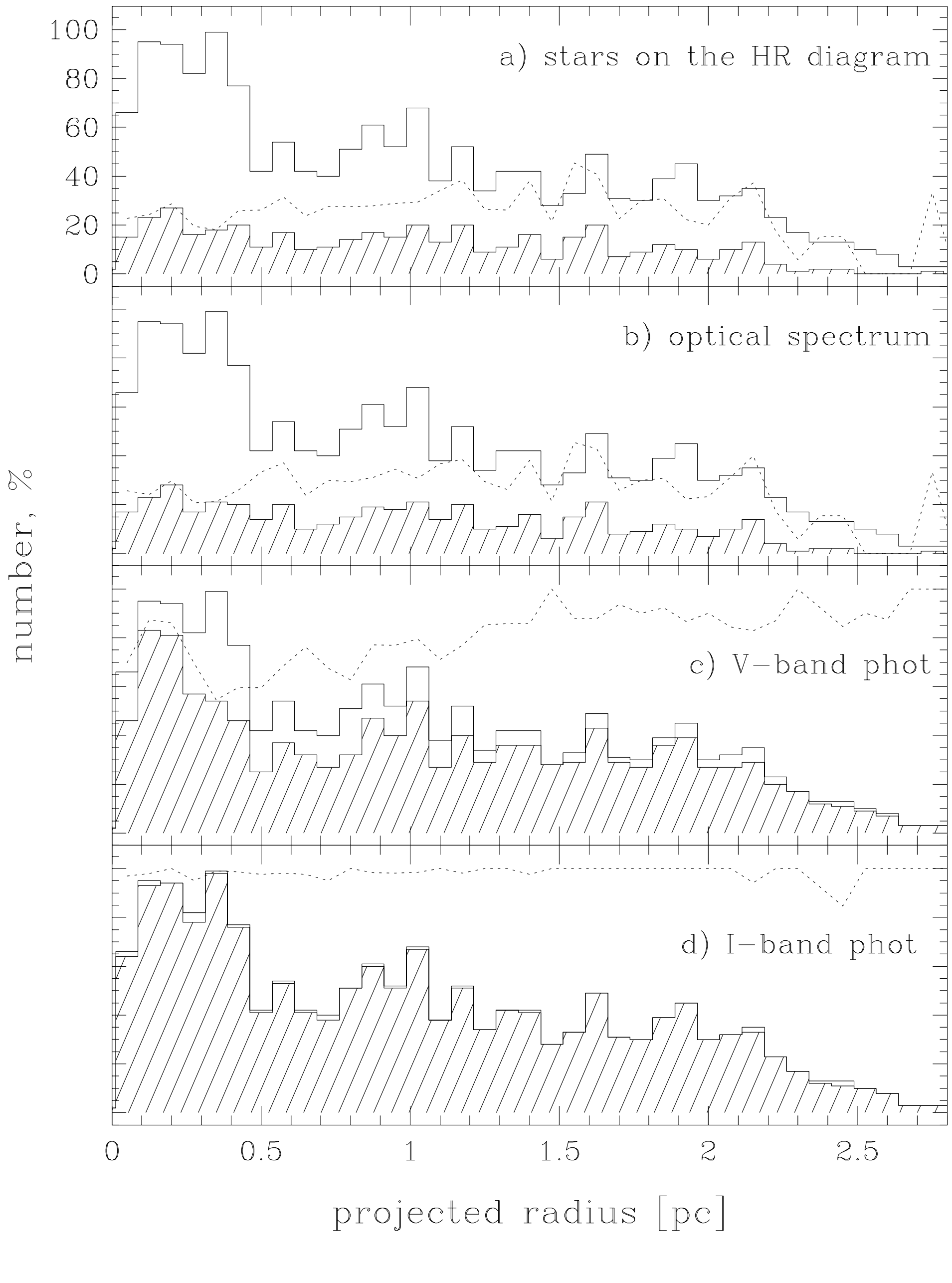

Fig. 2.— *Sample completeness with projected radius.* The open histogram indicates the radial distribution of stellar sources identified at I-band, and is the same on all five panels. The hatched histogram indicates the distribution of sources which appear on our HR diagram (panel a), with optical spectral types (panel b), with V-band photometry (panel c), with I-band photometry (panel d; note that not all identified point sources have photometric measurements), and with K-band photometry (panel e). The dotted line in each panel indicates the fractional completeness, which is $\sim 30\%$ and roughly uniform with projected cluster radius for stars able to be located on the HR diagram (top panel).

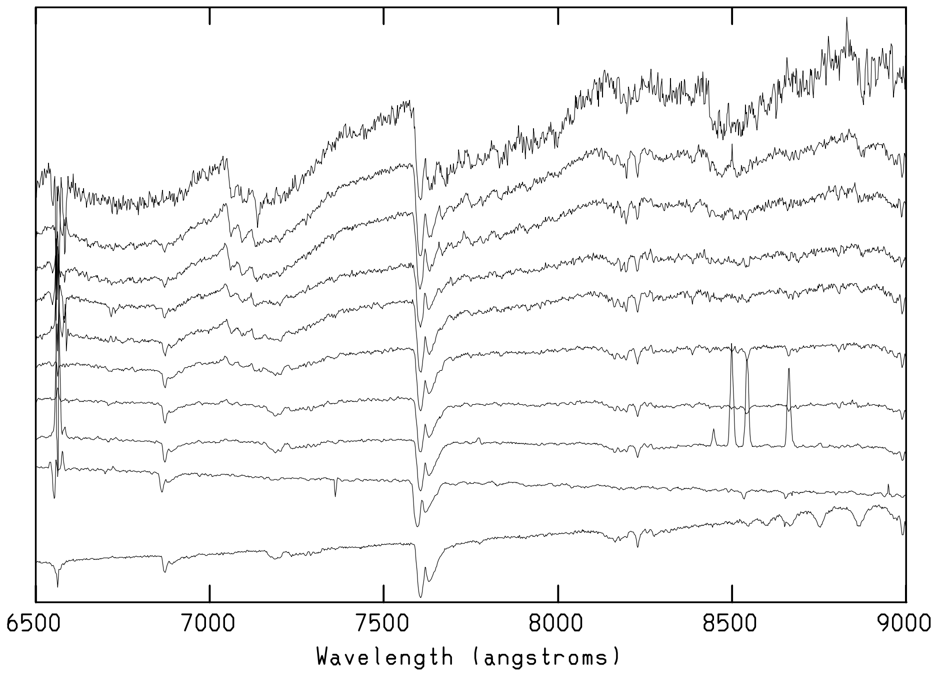

Fig. 3.— *Sample of ONC spectra from HYDRA and RCSP.*

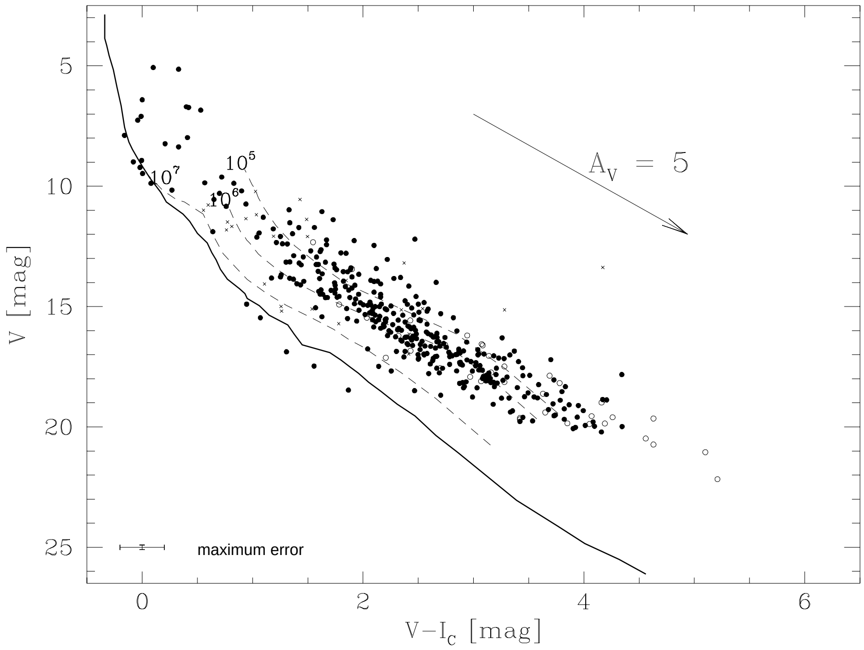

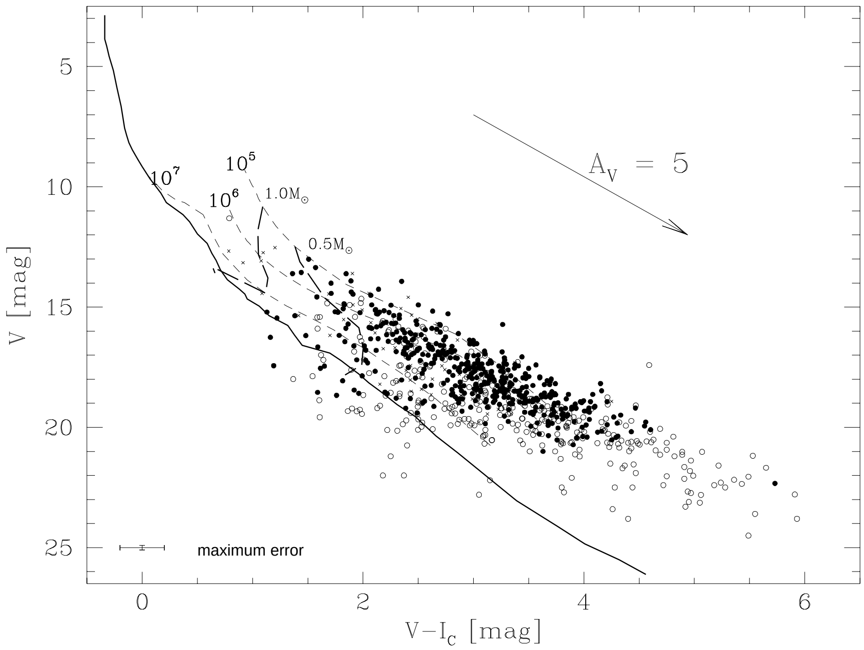

Fig. 4.— *Color-magnitude diagram for stars located on (panel a) and not yet located on (panel b) the HR diagram.* All stars with measured V- and I-band are shown along with the reddening vector corresponding to 5 magnitudes of visual extinction and the zero-age main sequence over the range O5-M7. The 0.1, 1, and 10Myr isochrones are from the calculations of D'Antona & Mazitelli (1994) . Filled circles indicate proper motion cluster members plus all sources which have been identified as being externally ionized; open circles indicate that no proper motion information is available; crosses indicate proper motion nonmembers.

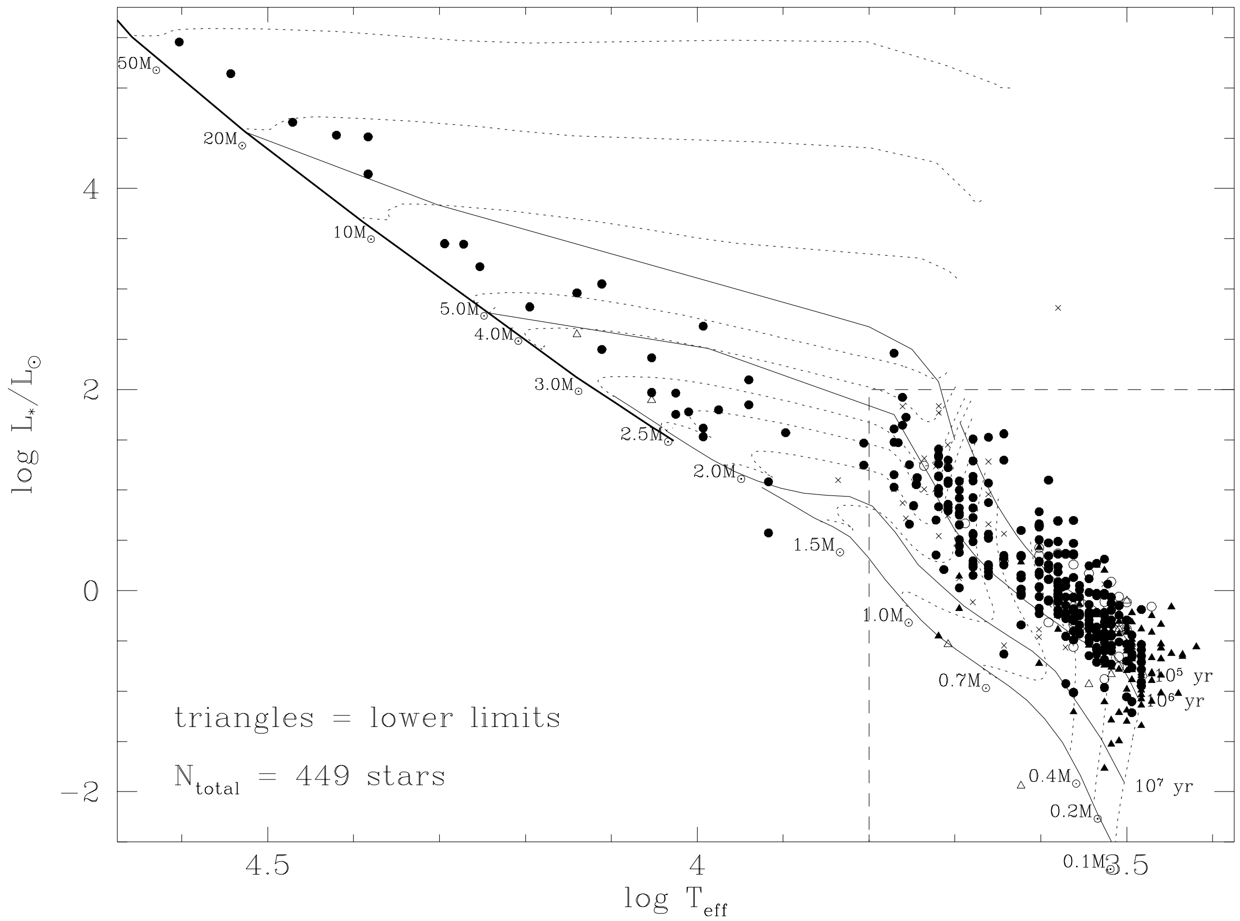

Fig. 5.— *HR diagram for the Orion Nebula Cluster.* Triangles indicate lower limits in luminosity. Filled circles/triangles indicate proper motion cluster members plus all sources which have been identified as being externally ionized; open circles/triangles indicate that no proper motion information is available; crosses indicate proper motion nonmembers. Superposed are the zero-age main sequence and the pre-main sequence evolutionary tracks of D'Antona & Mazitelli (1994, model 1); over the mass range from 0.1 $M_\odot$ to 2.5 $M_\odot$; Swenson *et al.* (1994, model F) from 4 $M_\odot$ to 5 $M_\odot$; and Ezer & Cameron (1967) from 10 $M_\odot$ to 50 $M_\odot$. The mean age of the optically visible stellar cluster is less then 1 Myr with an age spread from <0.1-2 Myr. The mass spectrum seems consistent with the Miller & Scalo (1979) mass spectrum. The trend of stellar increasing stellar age with mass suggests errors in the zero-point of the tracks, *i. e.* the initial mass-radius relationship with which the pre-main sequence evolutionary calculations begin. CaII emission is seen from ∼15% of the stars and excess emission at 2 μm is found in ∼45% of the stars represented on this Figure.

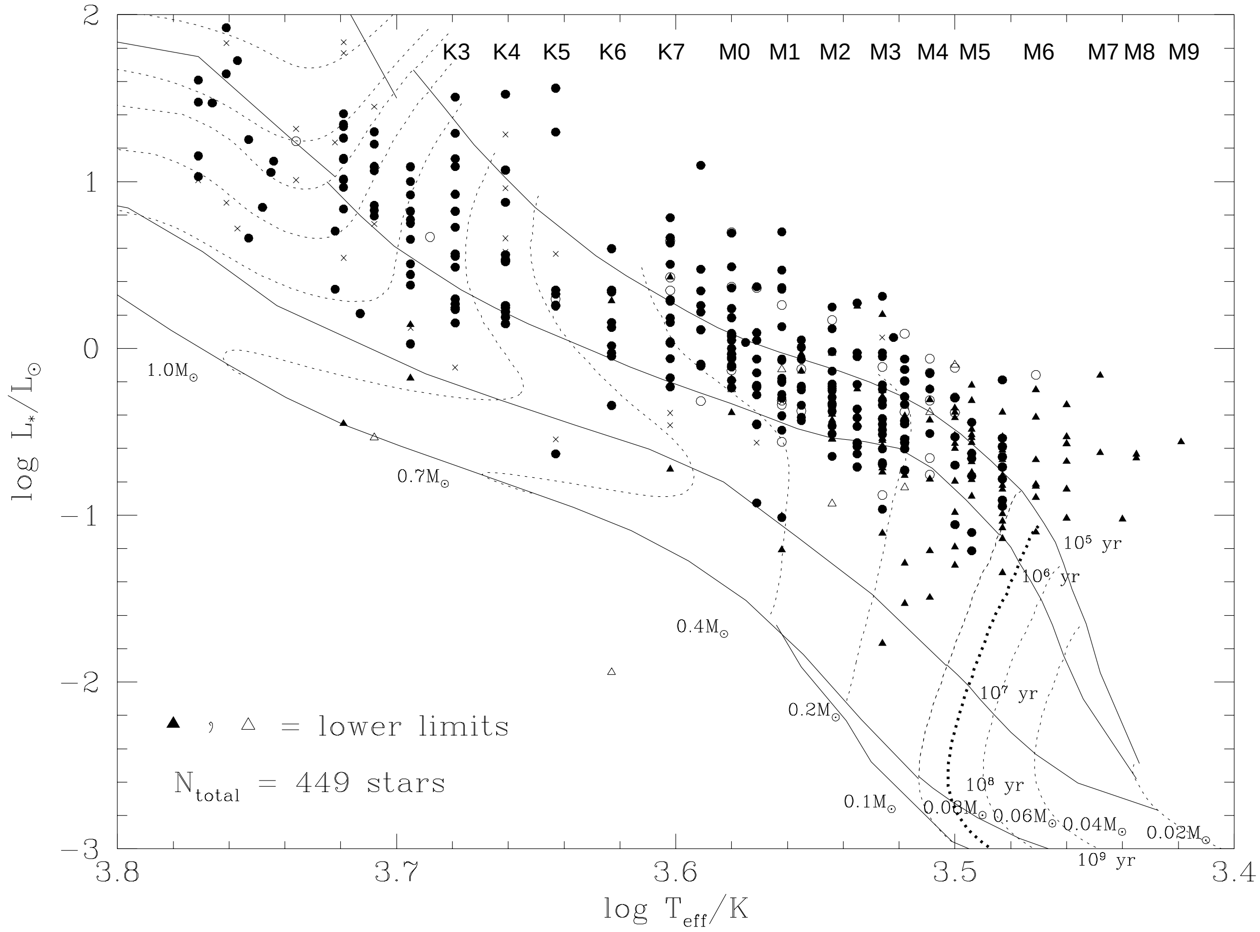

Fig. 6.— *Low-mass end of the HR diagram for the Orion Nebula Cluster.* All lines and symbols are the same as in Figure 5 with the pre-main sequence evolutionary calculations of D'Antona & Mazitelli now shown down to 0.02 $M_{\odot}$. Note the relative sparseness of the HR diagram between spectral types K5-K7, and also the locations of stars M6.5 and later relative to the tracks.

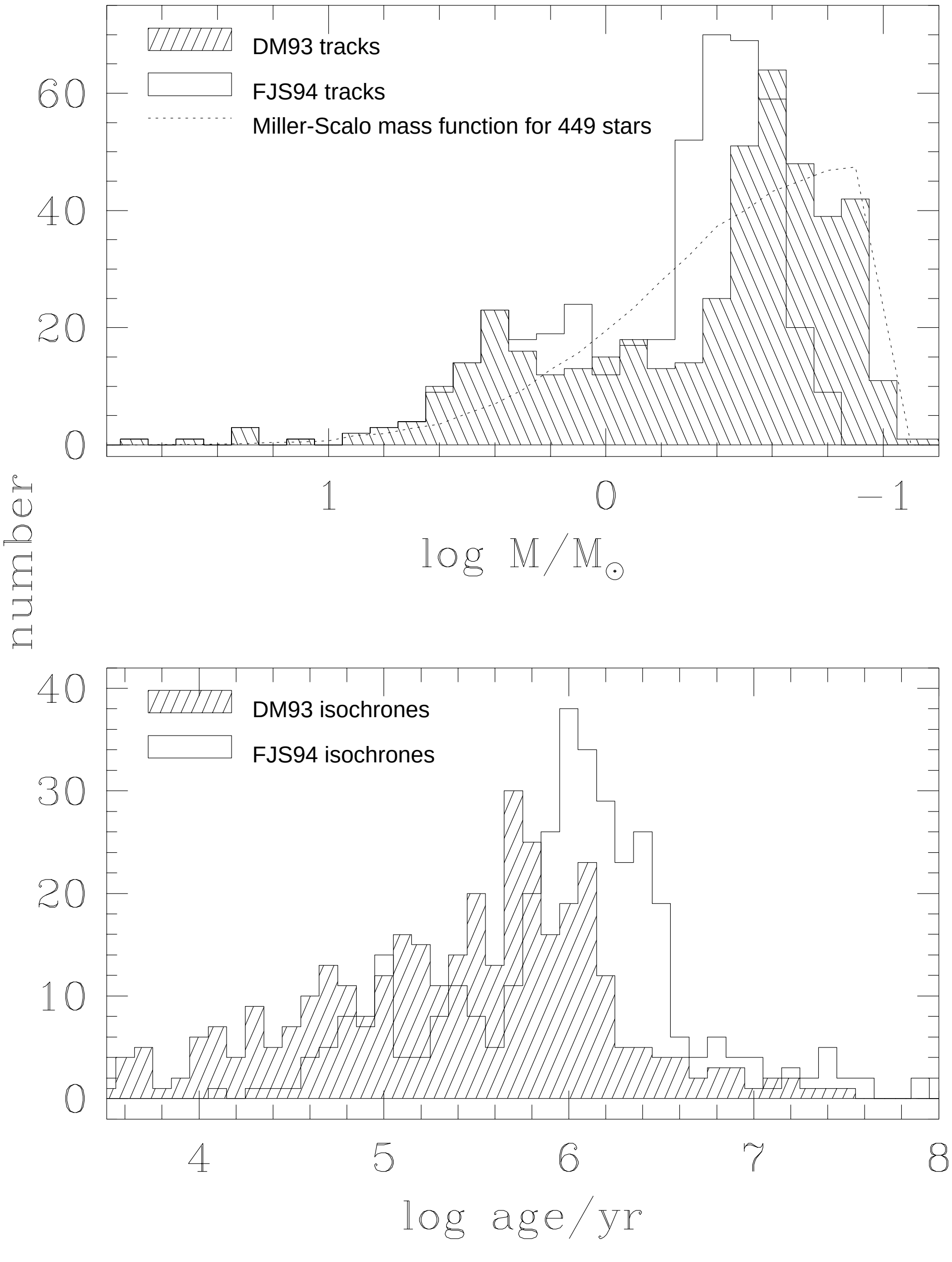

Fig. 7.— *Distribution of stellar masses (upper panel) and ages (lower panel;* $M < 1.5$ M$_\odot$ *only).* Filled histogram represents stellar parameters derived from the D'Antona & Mazitelli (1994) calculations while open histogram represents those from the Swenson, *et al.* (1994) calculations. The D'Antona & Mazitelli (1994) tracks and isochrones yield characteristically lower masses and younger ages than the Swenson, *et al.* (1994) predictions. In the top panel, the D'Antona & Mazitelli (1994) mass distribution is seen to peak around 0.3 M$_\odot$ and to fall off towards lower masses, in general agreement with the Miller & Scalo function; the Swenson, *et al.* (1994) mass distribution peaks around 0.4 M$_\odot$ and falls off quickly below this. In the bottom panel, the D'Antona & Mazitelli (1994) age distribution shows most (>50%) of the star formation to have occurred within the last 0.5 Myr and >85% within the last 2 Myr; according to the Swenson, *et al.* (1994) calculations, 1.5Myr passed before 50% of the stars were formed, with 4.5 Myr needed for 85% of the star formation to have occurred.

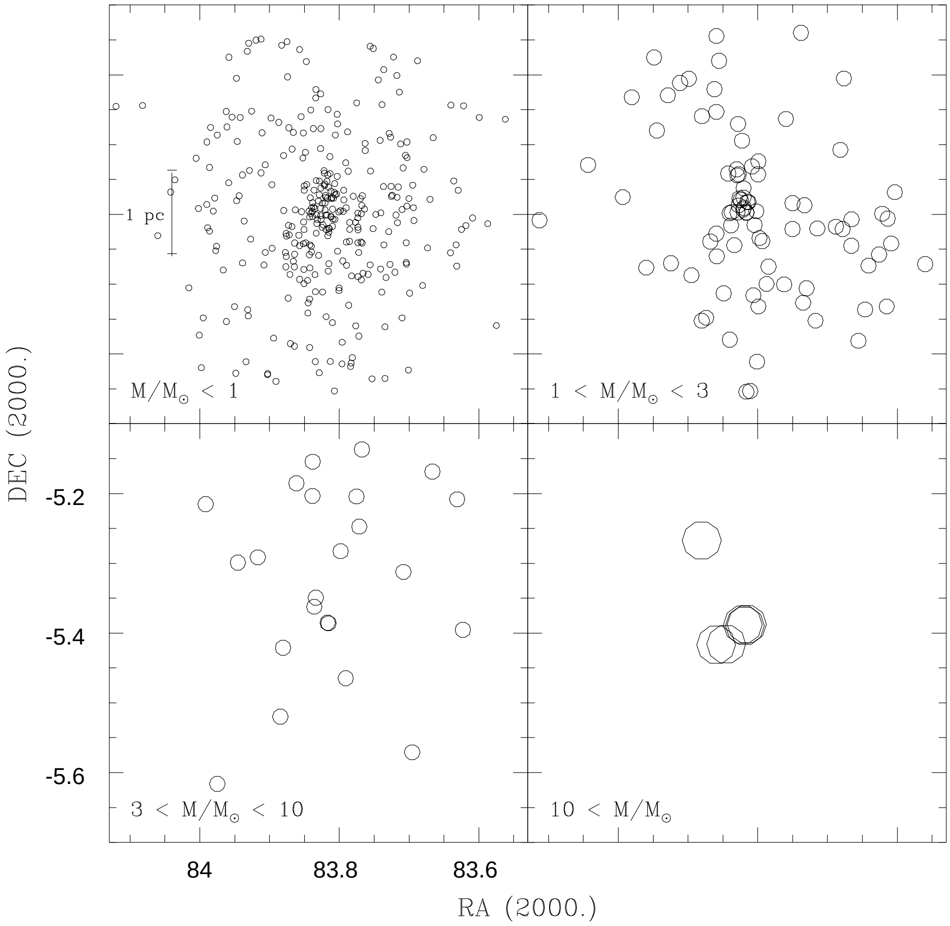

Fig. 8.— *Spatial distribution of stars of various mass.* Large, medium, and small symbols indicate $10 < M/M_\odot$, $1 < M/M_\odot < 10$, and $0.1 < M/M_\odot < 1$, respectively. Although the highest-mass and lowest-mass stars are clearly clustered towards the center of the distribution, intermediate-mass stars appear more uniformly distributed.

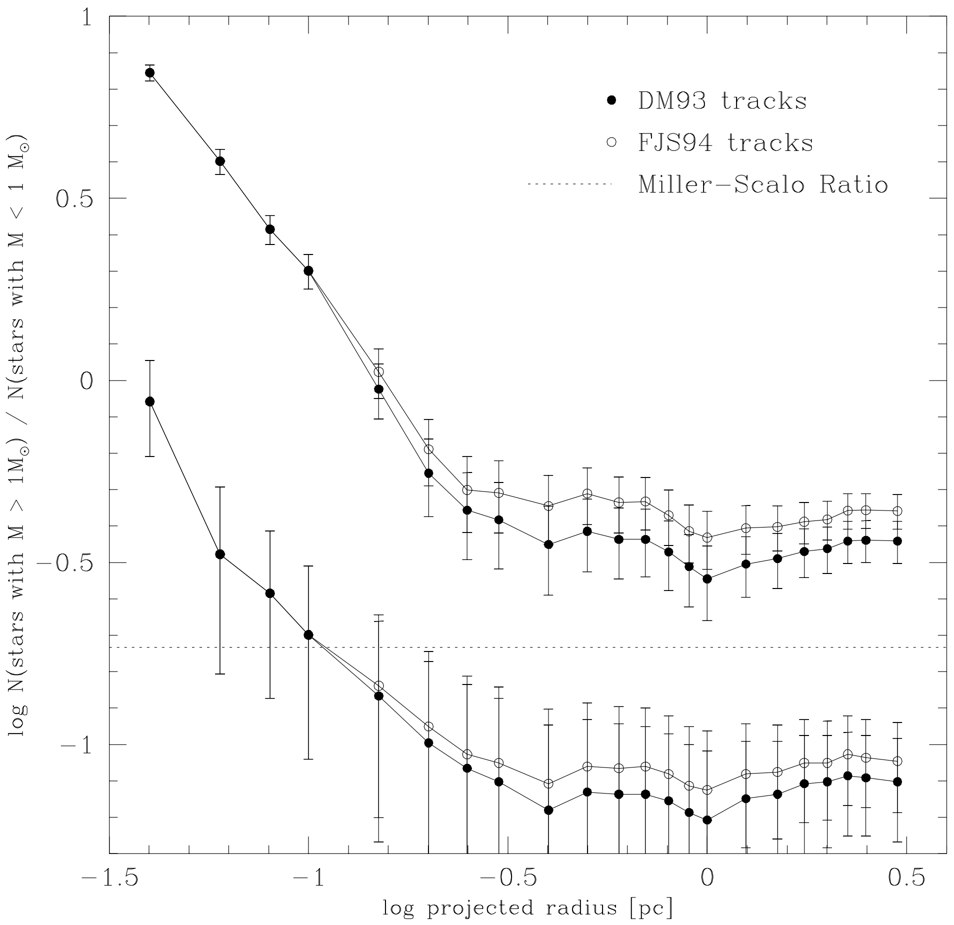

Fig. 9.— *Variation of the ratio of high-to-low-mass stars with projected radius.* Filled symbols represent the D'Antona & Mazitelli (1994) pre-main sequence evolutionary calculations; open symbols represent the Swenson, *et al.* (1994) caclulations. The horizontal dotted line is the ratio of high-to-low- mass stars predicted by Miller & Scalo (0.185) while the solid curves are the observed distributions including (top two lines) only stars located on the HR diagram and (bottom two lines) all stars in the ONC, assuming sub-solar masses for those not located on the HR diagram. Over the radial range 0.3-3pc, the ratio of high- to low-mass stars in the ONC is flat and consistent with the Miller & Scalo function to within our ability to constrain it. Inside of 0.3pc, however, the ratio rises sharply with decreasing radius and is clearly inconsistent with the Miller & Scalo function.

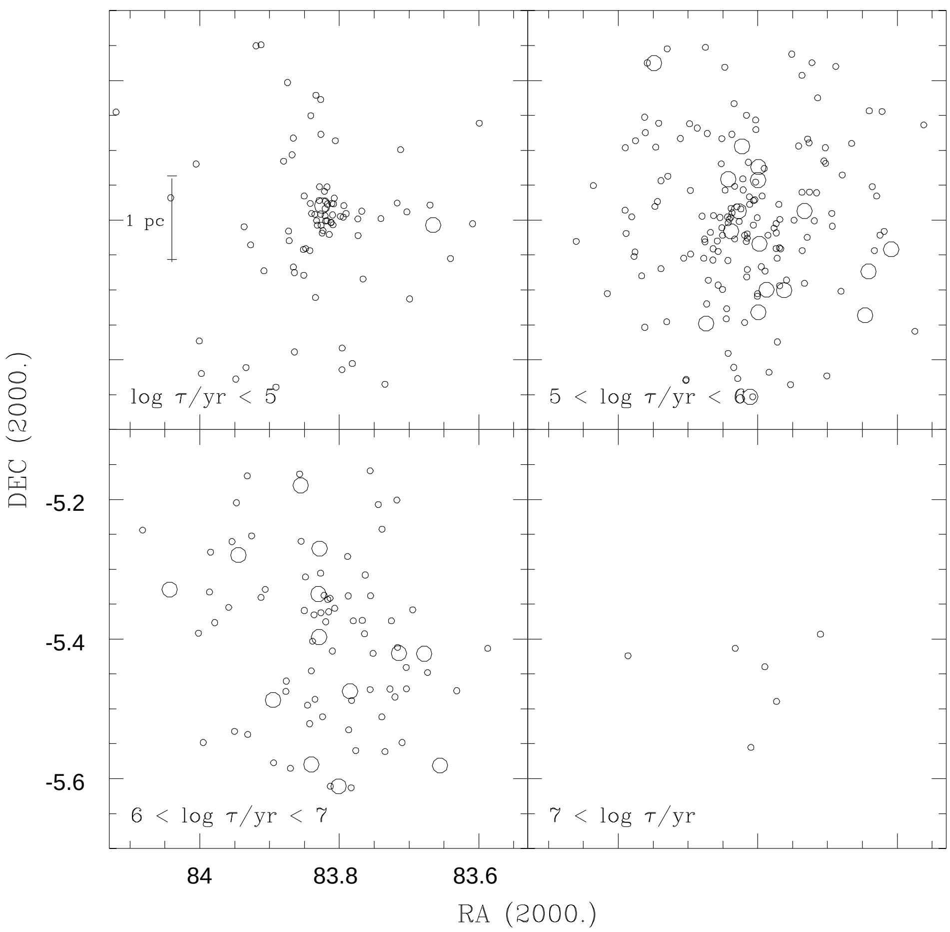

Fig. 10.— *Spatial distribution of stars of various age.* Only stars less massive than 1.5 $M_\odot$ are included. Medium and small symbols indicate $1 < M/M_\odot < 1.5$ and $0.1 < M/M_\odot < 1$, respectively. The youngest stars are clearly clustered towards the center of the distribution.

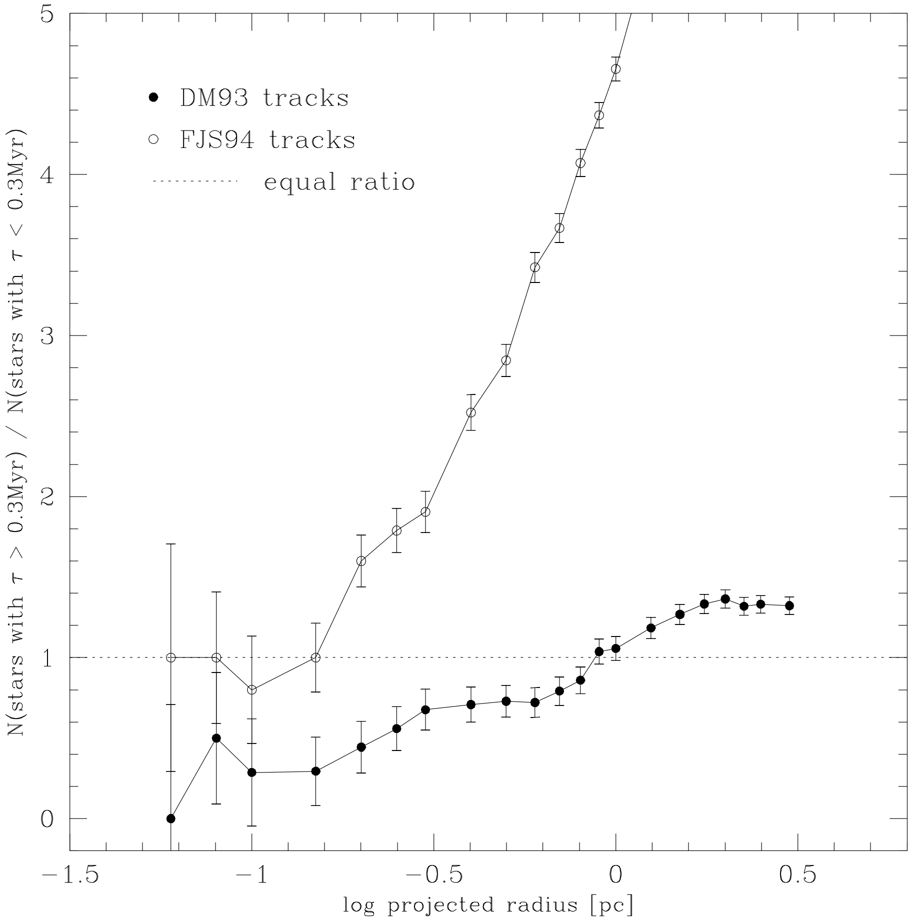

Fig. 11.— *Variation of the ratio of old-to-young stars with projected radius.* Only stars less massive than 1.5 $M_{\odot}$ are included. Filled symbols represent the D'Antona & Mazitelli (1994) pre-main sequence evolutionary calculations; open symbols represent the Swenson, *et al.* (1994) caclulations. The ratio of old-to-young stars in the ONC steadily increases with radius, *i. e.* the cluster center is dominated by the youngest stars.

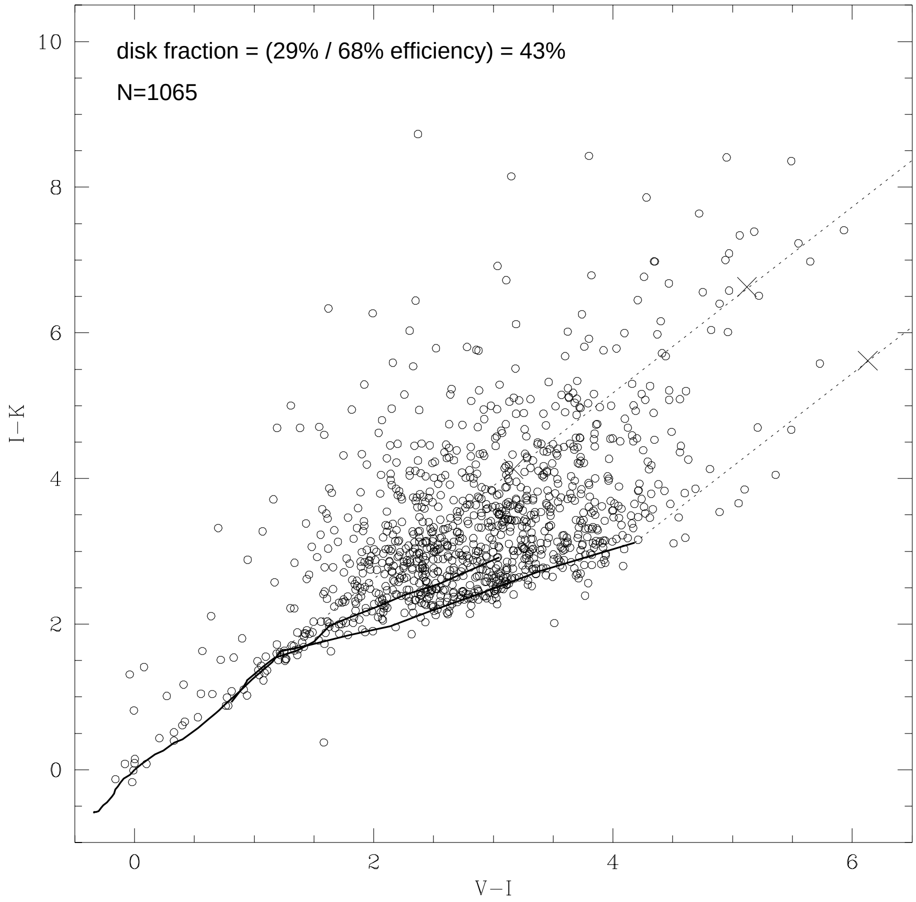

Fig. 12.— $(V - I_C) - (I_C - K)$ *color-color diagram for all ONC stars with V-, I-, and K-band photometry.* Heavy solid lines indicate the loci of colors expected for main sequence dwarfs and post-main sequence giants, while dotted lines drawn from the extrema of the dwarf and giant sequences are reddening vectors. Crosses mark intervals of 5 mag of visual extinction along the reddening vectors. Assuming an efficiency factor of this diagram in detecting stars with circumstellar material derived from our knowledge of the Taurus stellar population, the fraction of the ONC sample with 2 μm excesses is 43%.

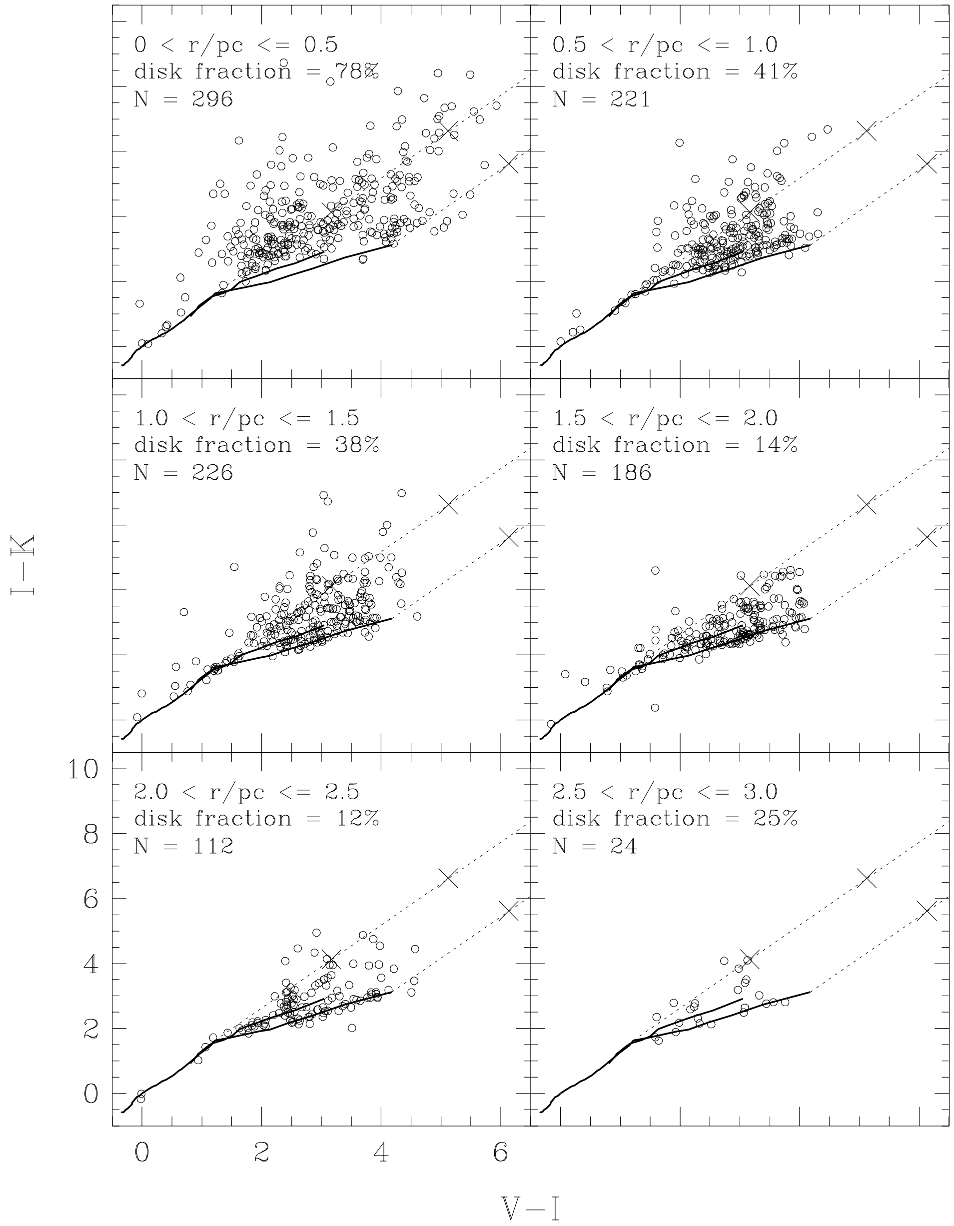

Fig. 13.— $(V-I_C)-(I_C-K)$ *color-color diagram as a function of projected cluster radius.* All lines and symbols are the same as in Figure 12. The disk fraction decreases with increasing radius from about 80% in the cluster center down to about 10% by a radius of 2.5pc.

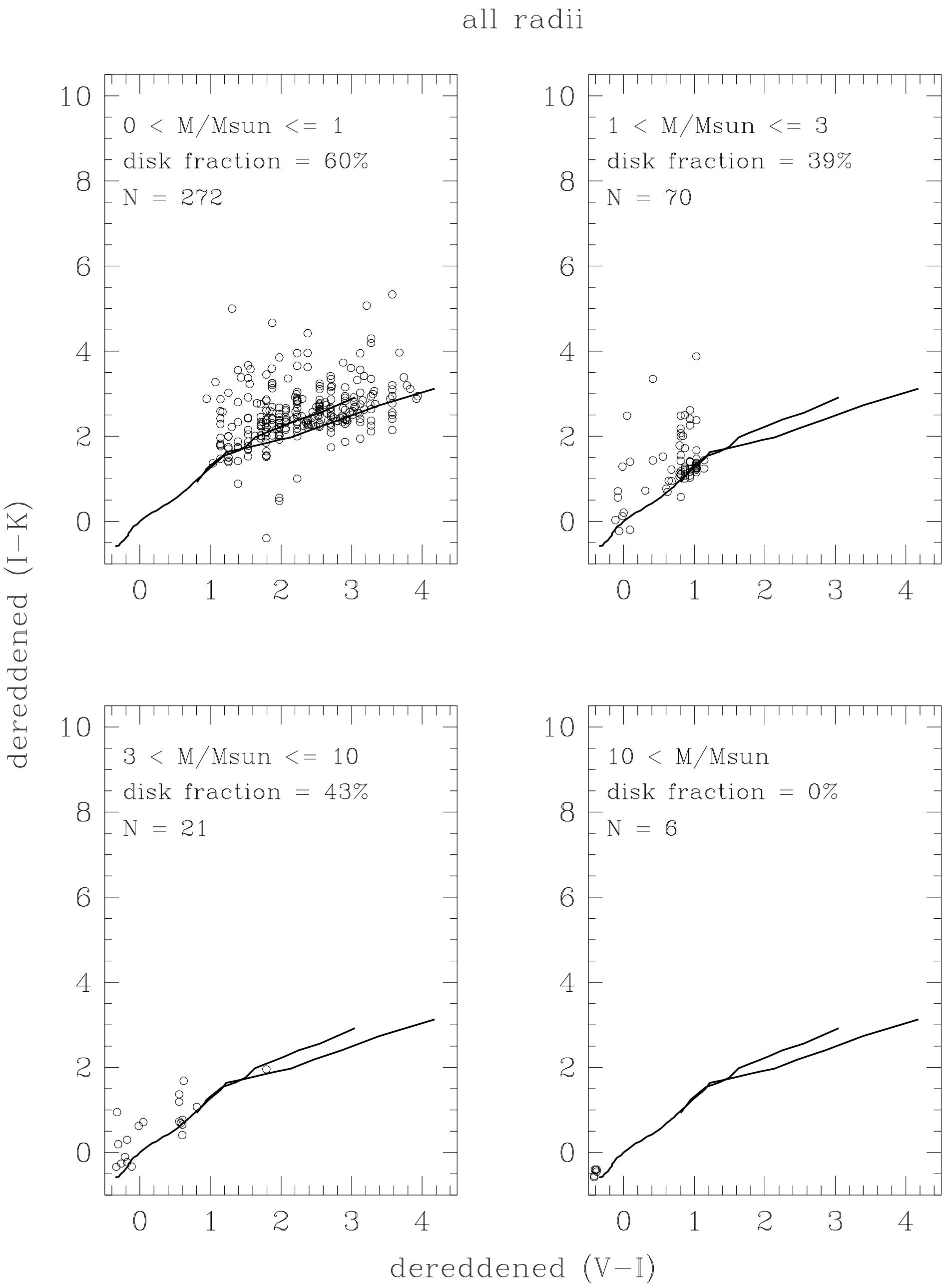

Fig. 14.— *De-reddened* $(V-I_C)-(I_C-K)$ *color-color diagram as a function of stellar mass.* Both the fraction of stars with $2\,\mu$m excesses and the magnitude of the excesses, decrease with increasing stellar mass.

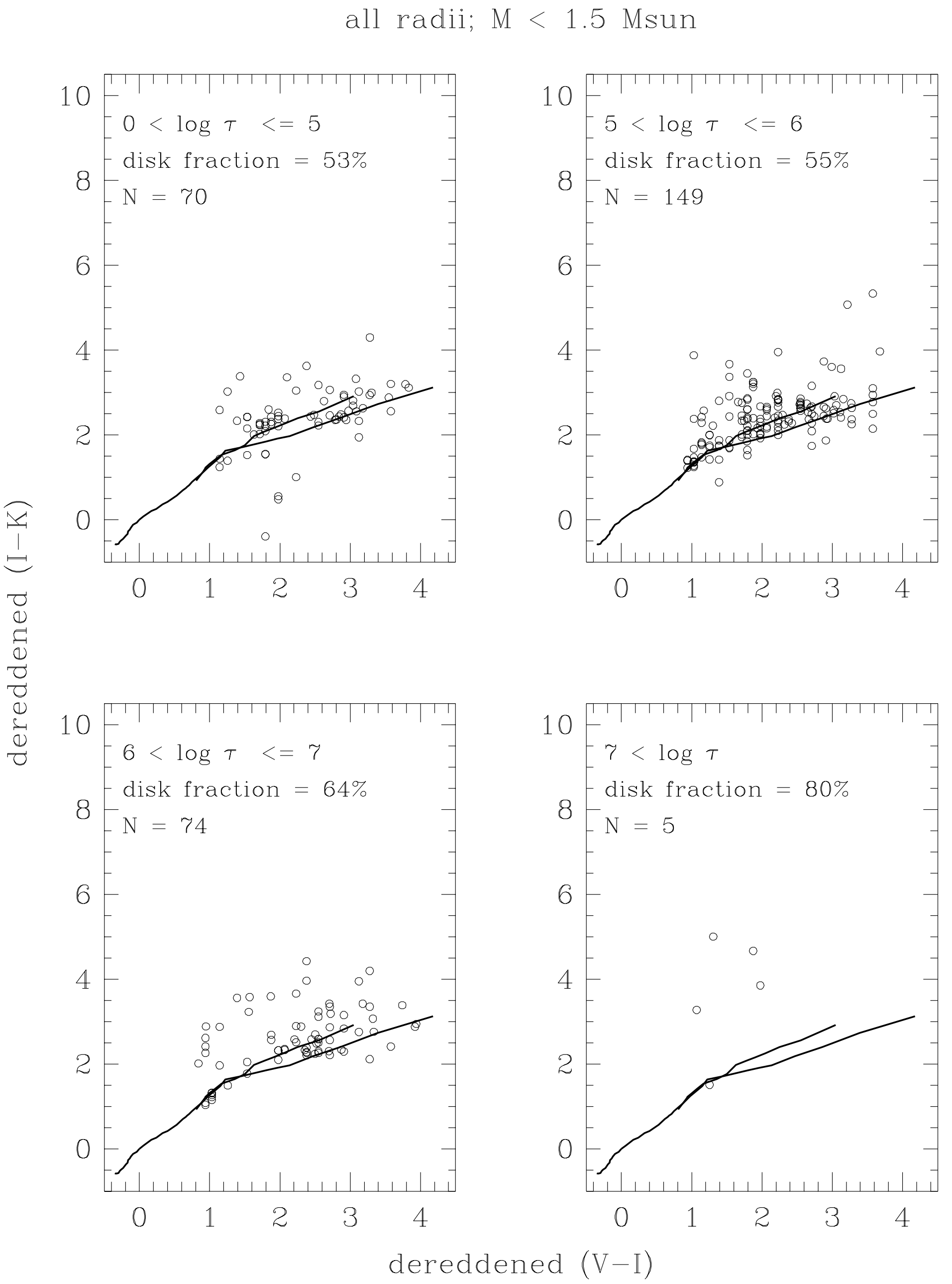

Fig. 15.— *De-reddened* $(V - I_C) - (I_C - K)$ *color-color diagram as a function of stellar age.* Only low-mass stars are included, to avoid the effects of the stellar birthline on age determinations. There is no apparent trend of near-infrared excess fraction with stellar age.